TECHNICAL REPORT

ISO/TR 13989-1

First edition
2000-03-15

Calculation of scuffing load capacity of cylindrical, bevel and hypoid gears —

Part 1:
Flash temperature method

Calcul de la capacité de charge au grippage des engrenages cylindriques, coniques et hypoïdes —

Partie 1: Méthode de la température-éclair

Reference number
ISO/TR 13989-1:2000(E)

ISO copyright office
Case postale 56 • CH-1211 Geneva 20
Tel. + 41 22 749 01 11
Fax + 41 22 734 10 79
E-mail copyright@iso.ch
Web www.iso.ch

Printed in Switzerland

Contents

Page

Foreword

ISO (the International Organization for Standardization) is a worldwide federation of national standards bodies (ISO member bodies). The work of preparing International Standards is normally carried out through ISO technical committees. Each member body interested in a subject for which a technical committee has been established has the right to be represented on that committee. International organizations, governmental and non-governmental, in liaison with ISO, also take part in the work. ISO collaborates closely with the International Electrotechnical Commission (IEC) on all matters of electrotechnical standardization.

The main task of technical committees is to prepare International Standards, but in exceptional circumstances a technical committee may propose the publication of a Technical Report of one of the following types:

— type 1, when the required support cannot be obtained for the publication of an International Standard, despite repeated efforts;

— type 2, when the subject is still under technical development or where for any other reason there is the future but not immediate possibility of an agreement on an International Standard;

— type 3, when a technical committee has collected data of a different kind from that which is normally published as an International Standard ("state of the art", for example).

Technical Reports of types 1 and 2 are subject to review within three years of publication, to decide whether they can be transformed into International Standards. Technical Reports of type 3 do not necessarily have to be reviewed until the data they provide are considered to be no longer valid or useful.

Technical Reports are drafted in accordance with the rules given in the ISO/IEC Directives, Part 3.

Attention is drawn to the possibility that some of the elements of this part of ISO/TR 13989 may be the subject of patent rights. ISO shall not be held responsible for identifying any or all such patent rights.

ISO/TR 13989-1, which is a Technical Report of type 2, was prepared by Technical Committee ISO/TC 60, *Gears*, Subcommittee SC 2, *Gear capacity calculation*.

This document is being issued in the Technical Report (type 2) series of publications (according to subclause G.3.2.2 of Part 1 of the ISO/IEC Directives, 1995) as a “prospective standard for provisional application” in the field of scuffing load capacity of gears because there is an urgent need for guidance on how standards in this field should be used to meet an identified need. In 1975, two methods to evaluate the risk of scuffing were documented to be studied by ISO/TC 60. It was agreed that after a period of experience one method shall be selected. Since the subject is still under technical development and there is a future possibility of an agreement on an International Standard, the publication of a type 2 Technical Report was proposed.

This document is not to be regarded as an “International Standard”. It is proposed for provisional application so that information and experience of its use in practice may be gathered. Comments on the content of this document should be sent to the ISO Central Secretariat.

A review of this Technical Report (type 2) will be carried out not later than three years after its publication with the options of: extension for another three years; conversion into an International Standard; or withdrawal.

ISO/TR 13989 consists of the following parts, under the general title *Calculation of scuffing load capacity of cylindrical, bevel and hypoid gears*:

— *Part 1: Flash temperature method*

— *Part 2: Integral temperature method*

Annexes A and B of this part of ISO 13989 are for information only.

Introduction

Since 1990 the flash temperature method, presented in this part of ISO/TR 13989, was enriched with research for short exposure times, consideration of transition diagrams, new approximations for the coefficient of friction, and completely renewed load sharing factors. In 1991 Prof. Blok contributed an extension of the flash temperature formula which made it directly applicable to hypoid gears.

The integral temperature, presented in ISO/TR 13989-2, averages the flash temperature and supplements empirical influence factors to the hidden load sharing factor. The resulting value approximates the maximum contact temperature, thus yielding about the same assessment of scuffing risk as the flash temperature method of this part of ISO/TR 13989. The integral temperature method is less sensitive for those cases where there are local temperature peaks, usually in gearsets that have low contact ratio or contact near the base circle or other sensitive geometries.

The risk of scuffing damage varies with the properties of gear materials, the lubricant used, the surface roughness of tooth flanks, the sliding velocities and the load. In contrast to the relatively long time of development of fatigue damage, one single momentary overload can initiate scuffing damage of such severity that affected gears may no longer be used. According to Blok [12][13][14][15][16][17], high contact temperatures of lubricant and tooth surfaces at the instantaneous contact position may effect a break-down of the lubricant film at the contact interface.

The interfacial contact temperature is conceived as the sum of two components:

— the interfacial bulk temperature of the moving interface, which, if varying, does so only comparatively slowly. For evaluating this component, it may be suitably averaged from the two overall bulk temperatures of the two rubbing teeth. The latter two bulk temperatures follow from the thermal network theory [18].

— the rapidly fluctuating flash temperature of the moving faces in contact. Special attention has to be paid to the coefficient of friction. A common practice is the use of a coefficient of friction valid for regular working conditions, although it may be stated that at incipient scuffing the coefficient of friction has significantly higher values.

The complex relationship between mechanical, hydrodynamical, thermodynamical and chemical phenomena was the objective of extensive research and experiments, which may induce various empirical influence factors. A direct suppletion of empirical influence factors may enforce the related functional factors in the main formula to be fixated to average values. However, correct treatment of functional factors (e.g. coefficient of friction, load sharing factor, thermal contact coefficient) keeps the main formula intact, in confirmation with the experiments and practice.

Next to the maximum contact temperature, the progress of the contact temperature along the path of contact provides necessary information to the gear design.

Calculation of scuffing load capacity of cylindrical, bevel and hypoid gears —

Part 1:
Flash temperature method

1 Scope

This part of ISO/TR 13989 specifies methods and formulae for evaluating the risk of scuffing, based on Blok's contact temperature concept.

The fundamental concept according to Blok is applicable to all machine elements with moving contact zones. The flash temperature formulae are valid for a band-shaped or approximately band-shaped Hertzian contact zone and working conditions characterized by sufficiently high Péclet numbers.

2 Normative references

The following normative documents contain provisions which, through reference in this text, constitute provisions of this part of ISO/TR 13989. For dated references, subsequent amendments to, or revisions of, any of these publications do not apply. However, parties to agreements based on this part of ISO/TR 13989 are encouraged to investigate the possibility of applying the most recent editions of the normative documents indicated below. For undated references, the latest edition of the normative document referred to applies. Members of ISO and IEC maintain registers of currently valid International Standards.

ISO 1122-1:1998, *Vocabulary of gear terms — Part 1: Definitions related to geometry*.

ISO 6336-1:1996, *Calculation of load capacity of spur and helical gears — Part 1: Basic principles, introduction and general influence factors*.

ISO 10300-1:—[1)], *Calculation of load capacity of bevel gears — Part 1: Introduction and general influence factors*.

ISO 10825:1995, *Gears — Wear and damage to gear teeth — Terminology*.

3 Terms, definitions, symbols and units

3.1 Terms and definitions

For the purposes of this part of ISO/TR 13989, the terms and definitions given in ISO 1122-1 and ISO 10825 apply.

3.2 Symbols and units

The symbols used in this part of ISO/TR 13989 are given in Table 1. The units of length metre, millimetre and micrometre are chosen in accordance with common practice. To achieve a "coherent" system, the units for B_M, c_γ, X_M are adapted to the mixed application of metre and millimetre or millimetre and micrometre.

1) To be published.

Table 1 — Symbols and units

Symbol	Description	Unit	Reference
a	centre distance	mm	Eq. (A.5)
b	facewidth, smaller value for pinion or wheel [a]	mm	Eq. (11)
b_{eff}	effective facewidth	mm	Eq. (12)
b_H	semi-width of Hertzian contact band	mm	Eq. (3)
B_M	thermal contact coefficient	N/(mm^{½}·m^{½}·s^{½}·K)	Eq (A.13)
B_{M1}	thermal contact coefficient of pinion	N/(mm^{½}·m^{½}·s^{½}·K)	Eq. (3)
B_{M2}	thermal contact coefficient of wheel	N/(mm^{½}·m^{½}·s^{½}·K)	Eq. (3)
C_{a1}	tip relief of pinion	µm	Eq. (48)
C_{a2}	tip relief of wheel	µm	Eq. (46)
C_{eff}	optimal tip relief	µm	Eq. (46)
C_{eq1}	equivalent tip relief of pinion	µm	Eq. (B.2)
C_{eq2}	equivalent tip relief of wheel	µm	Eq. (B.3)
C_{f1}	root relief of pinion	µm	Eq. (B.3)
C_{f2}	root relief of wheel	µm	Eq. (B.2)
c_{M1}	specific heat per unit mass of pinion	J/(kg·K)	Eq. (9)
c_{M2}	specific heat per unit mass of wheel	J/(kg·K)	Eq. (10)
c_γ	mesh stiffness	N/(mm·µm)	Eq. (B.1)
d_1	reference diameter of pinion	mm	Eq. (34)
d_2	reference diameter of wheel	mm	Eq. (35)
d_{a1}	tip diameter of pinion	mm	Eq. (34)
d_{a2}	tip diameter of wheel	mm	Eq. (35)
E_1	modulus of elasticity of pinion	N/mm^2	Eq. (A.10)
E_2	modulus of elasticity of wheel	N/mm^2	Eq. (A.10)
E_r	reduced modulus of elasticity	N/mm^2	Eq. (A.9)
F_{ex}	external axial force	N	Eq. (18)
F_n	normal load in wear test	N	Fig. 1
F_t	nominal tangential force	N	Eq. (11)
H_1	auxiliary dimension	mm	Eq. (B.3)
H_2	auxiliary dimension	mm	Eq. (B.2)
h_{am1}	tip height in mean cone of pinion	mm	Eq. (43)
h_{am2}	tip height in mean cone of wheel	mm	Eq. (44)

Table 1 — Symbols and units *(continued)*

Symbol	Description	Unit	Reference
K_A	application factor	—	Eq. (11)
$K_{B\alpha}$	transverse load factor (scuffing)	—	Eq. (11)
$K_{B\beta}$	face load factor (scuffing)	—	Eq. (11)
$K_{H\alpha}$	transverse load factor (contact stress)	—	Eq. (15)
$K_{H\beta}$	face load factor (contact stress)	—	Eq. (14)
K_{mp}	multiple path factor	—	Eq. (11)
K_v	dynamic factor	—	Eq. (11)
m_n	normal module	mm	Eq. (B.2)
n_1	revolutions per minute of pinion	r/min	Eq. (5)
n_p	number of mesh contacts	—	Eq. (16)
Pe_1	Péclet number of pinion material	—	Eq. (9)
Pe_2	Péclet number of wheel material	—	Eq. (10)
Q	quality grade	—	Eq. (57)
Ra_1	tooth flank surface roughness of pinion	µm	Eq. (28)
Ra_2	tooth flank surface roughness of wheel	µm	Eq. (28)
R_m	cone distance of mean cone	mm	Eq. (A.16)
r_{m1}	reference radius in mean cone of pinion	mm	Eq. (43)
r_{m2}	reference radius in mean cone of wheel	mm	Eq. (44)
S_B	safety factor for scuffing	—	Eq. (100)
S_{FZG}	load stage (in FZG test)	—	Eq. (99)
t_1	contact exposure time of pinion	µs	Eq. (95)
t_2	contact exposure time of wheel	µs	Eq. (96)
t_c	contact exposure time at bend of curve	µs	Eq. (97)
t_{max}	longest contact exposure time	µs	Eq. (95)
u	gear ratio	—	Eq. (A.6)
u_v	virtual ratio	—	Eq. (B.6)
v_g	sliding velocity	m/s	Fig. 1
v_{g1}	tangential velocity of pinion	m/s	Eq. (3)
v_{g2}	tangential velocity of wheel	m/s	Eq. (3)
$v_{g\Sigma C}$	sum of tangential velocities in pitch point	m/s	Eq. (25)
v_t	pitch line velocity	m/s	Eq. (26)
w_{Bn}	normal unit load	N/mm	Eq. (3)
w_{Bt}	transverse unit load	N/mm	Eq. (5)

Table 1 — Symbols and units *(continued)*

Symbol	Description	Unit	Reference
X_{but}	buttressing factor	—	Eq. (54)
X_{butA}	buttressing value	—	Eq. (51)
X_{butE}	buttressing value	—	Eq. (51)
X_G	geometry factor	—	Eq. (A.5)
X_J	approach factor	—	Eq. (3)
X_L	lubricant factor	—	Eq. (25)
X_M	thermo-elastic factor	$K \cdot N^{-¾} \cdot s^{-½} \cdot m^{-½} \cdot mm$	Eq. (5)
X_{mp}	multiple mating pinion factor	—	Eq. (22)
X_R	roughness factor	—	Eq. (25)
X_S	lubrication system factor	—	Eq. (22)
X_W	structural factor	—	Eq. (94)
$X_{\alpha\beta}$	angle factor	—	Eq. (A.6)
X_Γ	load sharing factor	—	Eq. (3)
X_Θ	gradient of the scuffing temperature	—	Eq. (97)
z_1	number of teeth of pinion	—	Eq. (30)
z_2	number of teeth of wheel	—	Eq. (30)
α_{a1}	transverse tip pressure angle of pinion	°	Eq. (31)
α_{a2}	transverse tip pressure angle of wheel	°	Eq. (30)
α_t	transverse pressure angle	°	Eq. (34)
α_{wn}	normal working pressure angle	°	Eq. (A.2)
α_{wt}	transverse working pressure angle	°	Eq. (7)
α_{y1}	pinion pressure angle at arbitrary point	°	Eq. (29)
β	helix angle	°	Eq. (18)
β_b	base helix angle	°	Eq. (49)
β_{bm}	base helix angle in midcone	°	Eq. (50)
β_w	working helix angle	°	Eq. (A.2)
Γ_A	parameter on the line of action at point A	—	Eq. (24)
Γ_{AA}	parameter on the line of action at point AA	—	Eq. (68)
Γ_{AB}	parameter on the line of action at point AB	—	Eq. (66)
Γ_{AU}	parameter on the line of action at point AU	—	Eq. (49)
Γ_B	parameter on the line of action at point B	—	Eq. (31)
Γ_{BB}	parameter on the line of action at point BB	—	Eq. (70)
Γ_D	parameter on the line of action at point D	—	Eq. (32)
Γ_{DD}	parameter on the line of action at point DD	—	Eq. (72)
Γ_{DE}	parameter on the line of action at point DE	—	Eq. (67)

Table 1 — Symbols and units *(continued)*

Symbol	Description	Unit	Reference
Γ_E	parameter on the line of action at point E	—	Eq. (24)
Γ_{EE}	parameter on the line of action at point EE	—	Eq. (74)
Γ_{EU}	parameter on the line of action at point EU	—	Eq. (49)
Γ_M	parameter on the line of action at point M	—	Eq. (86)
Γ_y	parameter on the line of action at arbitrary point	—	Eq. (7)
γ_1	angle of direction of tangential velocity of pinion	—	Eq. (3)
γ_2	angle of direction of tangential velocity of wheel	—	Eq. (3)
δ_1	pitch cone angle of pinion	°	Eq. (37)
δ_2	pitch cone angle of wheel	°	Eq. (39)
ε_α	transverse contact ratio	—	Eq. (76)
ε_β	overlap ratio	—	Eq. (52)
η_{oil}	absolute (dynamic) viscosity at oil temperature	mPa·s	Eq. (27)
Θ_B	contact temperature	°C	Eq. (1)
Θ_{Bmax}	maximum contact temperature	°C	Eq. (2)
Θ_{fl}	flash temperature	K	Eq. (1)
Θ_{flm}	average flash temperature	K	Eq. (22)
Θ_{flmax}	maximum flash temperature	K	Eq. (2)
Θ_{flmaxT}	maximum flash temperature at test	K	Eq. (94)
Θ_M	bulk temperature	°C	Eq. (22)
Θ_{Mi}	interfacial bulk temperature	°C	Eq. (1)
Θ_{M1}	bulk temperature of pinion teeth	°C	Eq. (20)
Θ_{M2}	bulk temperature of wheel teeth	°C	Eq. (20)
Θ_{MT}	bulk temperature at test	°C	Eq. (94)
Θ_{oil}	oil temperature before reaching the mesh	°C	Eq. (22)
Θ_S	scuffing temperature	°C	Eq. (94)
Θ_{Sc}	scuffing temperature at long contact time	°C	Eq. (97)
λ_{M1}	heat conductivity of pinion	N/(s·K)	Eq. (9)
λ_{M2}	heat conductivity of wheel	N/(s·K)	Eq. (10)
μ	coefficient of friction in pin-and-ring test	—	Fig. 1
μ_m	mean coefficient of friction	—	Eq. (3)
ν_1	Poisson's ratio of pinion material	—	Eq. (A.10)
ν_2	Poisson's ratio of wheel material	—	Eq. (A.10)

Table 1 — Symbols and units *(concluded)*

Symbol	Description	Unit	Reference
ρ_{M1}	density of pinion material	kg/m³	Eq. (9)
ρ_{M2}	density of wheel material	kg/m³	Eq. (10)
ρ_{relC}	relative radius of curvature at pitch point	mm	Eq. (25)
ρ_{y1}	radius of curvature at arbitrary point of pinion	mm	Eq. (5)
ρ_{y2}	radius of curvature at arbitrary point of wheel	mm	Eq. (5)
ρ_{yrel}	relative radius of curvature at arbitrary point	mm	Eq. (5)
Σ	shaft angle	°	Eq. (A.15)
Φ	quill shaft twist	°	Eq. (17)

a The term wheel is used for the mating gear of a pinion.

4 Scuffing and wear

4.1 Occurrence of scuffing and wear

When gear teeth are completely separated by a full fluid film of lubricant, there is no contact between the asperities of the tooth surfaces, and usually there is no scuffing or wear. Here, the coefficient of friction is rather low. In exceptional cases a damage similar to scuffing may be caused by a sudden thermal instability [19] in a thick oil film, which phenomenon is not treated here.

For thinner elastohydrodynamic films, incidental asperity contact takes place. As the mean film thickness decreases, the number of contacts increases acccordingly. Abrasive wear, adhesive wear or scuffing becomes possible. Abrasive wear may occur due to the rolling action of the gear teeth or the presence of abrasive particles in the lubricant. Adhesive wear occurs by localized welding and subsequent detachment and transfer of particles from one or both of the meshing teeth. Abrasive or adhesive wear may not be harmful if it is mild and if it subsides with time, as in a normal run-in process.

In contrast to mild wear, scuffing is a severe form of adhesive wear that can result in progressive damage to the gear teeth. In contrast to pitting and fatigue breakage which show a distinct incubation period, a short transient overloading can result in scuffing failure.

Excessive aeration or the presence in the lubricant of contaminants such as metal particles in suspension, or water, also increases the risk of scuffing damage. After scuffing, high speed gears tend to suffer high levels of dynamic loading due to vibration which usually cause further damage by scuffing, pitting or tooth breakage.

In most cases, the resistance of gears to scuffing can be improved by using a lubricant with enhanced anti-scuff[2)] additives. It is important, however, to be aware that some disadvantages attend the use of anti-scuff additives: corrosion of copper, embrittlement of elastomers, lack of world-wide availability, etc.

The methods described are not suitable for "cold scuffing" which is in general associated with low speed, under approx. 4 m/s, through-hardened heavily loaded gears of rather poor quality.

4.2 Transition diagram

The lubrication condition of sliding concentrated steel contacts, which operate in a liquid lubricant, can be described [20][21][22][23] in terms of transition diagrams. A transition diagram according to Figure 1 is considered to be applicable to contacts functioning at constant oil bath temperature.

2) The less correct designation Extreme Pressure, EP, is replaced by anti-scuff.

At combinations of normal force F_n and relative sliding velocity v_g which fall below the line A1-S, in region I, see Figure 1, the lubrication condition is characterized by a coefficient of friction of about 0,1 and a specific wear rate of 10^{-2} mm³/(N·m) to 10^{-6} mm³/(N·m) (i.e. volume wear per unit of normal force, per unit of sliding distance).

If, with v_g not above a value according to point S, the load is increased into region II, a transition into a second condition of lubrication occurs. This mild wear lubrication condition is characterized by a coefficient of friction of about 0,3 to 0,4 and a specific wear rate of 1 mm³/(N·m) to 5 mm³/(N·m).

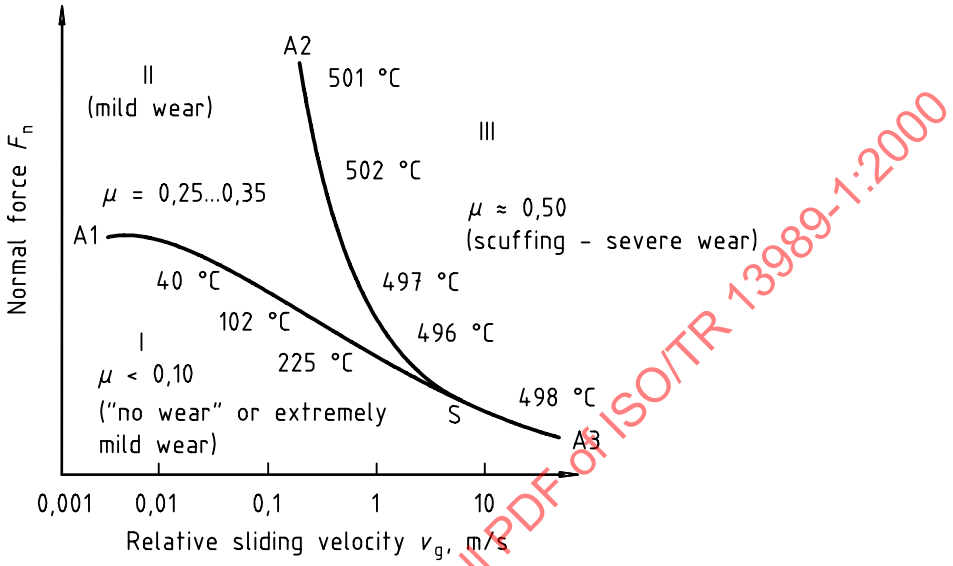

Figure 1 — Transition diagram for contraform contacts with example of calculated contact temperatures

If load is increased still further, a transition into a third condition of lubrication, region III, occurs at intersection of the line A2-S. This region is characterized by a coefficient of friction equal to 0,4 to 0,5. The wear rate, however, is considerably higher, i.e. 100 mm³/(N·m) to 1 000 mm³/(N·m), than in regions I and II and the worn surfaces show evidence of severe wear in the form of scuffing. If load increases at relative sliding velocities beyond point S, a direct transition from region I to region III takes place.

There is strong evidence that the position of the line A1-S-A3 depends upon lubricant viscosity [24] as well as upon Hertzian contact pressure [20][21]. At combinations of F_n and v_g that fall below this line, it is believed that the surfaces are kept apart by a thin lubricant film which is, however, penetrated by roughness asperities. In this context, the term "partial elastohydrodynamic lubrication" has been used [21].

In region III liquid film effects are completely absent. This region is identical to the region of "incipient scuffing" [25]. There is evidence that the transition which occurs at intersecting the line A2-S is associated with reaching a critical value of the contact temperature. This is the fundamental concept according to Blok.

The transition diagram shown is applicable to newly assembled, i.e. unoxidized steel contacts, as occur in gears, cams and followers, etc. It has been found that the diagram is applicable to four-ball as well as to pin-and-ring test results.

Along curve A1-S-A3 temperature ranges from an oil bath, respectively overall bulk, respectively interfacial bulk temperature, of 28 °C at v_g = 0,001 m/s to a contact temperature of 498 °C at v_g = 10 m/s. This temperature behaviour strongly suggests that the collapse of (partial) elasto-hydrodynamical lubrication does not occur at a constant contact or interfacial bulk temperature, for instance being associated with melting of chemisorbed material. Instead, the pronounced decrease of load carrying capacity with increasing sliding velocity is supposed to be due to decreasing viscosity [24][26][27][28][29].

Contrary to the above, calculated contact temperatures along curve A2-S-A3 tend to attain a constant value, e.g. in the case of AISI 52100 steel specimens approximately 500 °C; see Figure 1. This suggests that the II-III transition is associated with a transformation in the steel, causing the wear mechanism of surfaces to change from mildly adhesive to severely adhesive, perhaps involving a mechanism of thermo-elastic instability [30][31].

Therefore, the results indicate scuffing is associated with a critical magnitude of the contact temperature. For steel, lubricated with mineral oils, the critical magnitude does not depend on load, velocity and geometry, and equals near 500 °C.

4.3 Friction at incipient scuffing

As shown in the transition diagram, Figure 1, in the case of scuffing the coefficient of friction leaps from about 0,25 to about 0,5. The corresponding contact temperature proves to be about 500 °C. This contact temperature is the sum of a measured interfacial bulk temperature of 28 °C and a calculated flash temperature of 470 °C. During the flash temperature calculation use is made of the coefficient of friction just before transition, $\mu = 0{,}35$. If this method has to be applied not only for pin-and-ring tests but also (during the design stage) for gear transmissions, one shall agree upon the choice of the value of the critical magnitude of the contact temperature on one hand and the value of the coefficient of friction to be used in the calculations on the other.

A gear load capacity can be predicted

— on the safe side, with the coefficient of friction $\mu = 0{,}50$;

— accurately, with the coefficient of friction between $\mu = 0{,}25$ and $\mu = 0{,}35$, dependent on the lubricant;

— according to previous practice, with a low coefficient of friction of regular working conditions, provided that the limiting contact temperature is correspondingly low.

In terms of previous practice, for non-additive and low-additive mineral oils, each combination of oil and rolling materials has a critical scuffing temperature which, in general, is constant regardless of the operating conditions, load, velocity and geometry.

For high-additive and certain kinds of synthetic lubricants the critical scuffing temperature may well vary from one set of operating conditions to another. So, this critical temperature must then be determined for each such set separately from tests which closely simulate the operating condition of the gearset.

5 Basic formulae

5.1 Contact temperature

As already mentioned in the introduction, the contact temperature is the sum of the interfacial bulk temperature, Θ_{Mi}, see 5.3, and the flash temperature, Θ_{fl}, see 5.2,

$$\Theta_B = \Theta_{Mi} + \Theta_{fl} \quad (1)$$

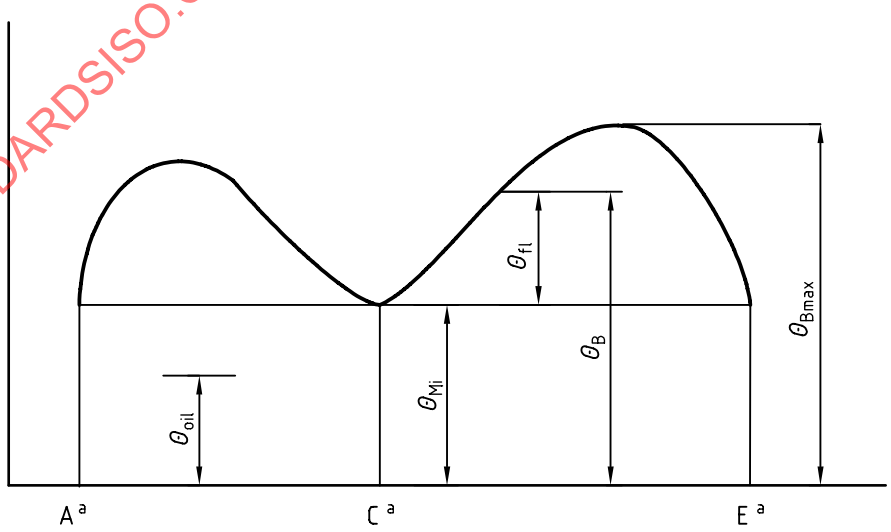

a Position in the path of contact.

Figure 2 — Contact temperature along the path of contact

Only the flash temperature varies along the path of contact; see Figure 2.

The maximum contact temperature is

$$\Theta_{Bmax} = \Theta_{Mi} + \Theta_{flmax} \tag{2}$$

where Θ_{flmax} is the maximum value of Θ_{fl}, being located either at the approach path or at the recess path.

Prediction of the probability of scuffing is possible by comparing the calculated maximum contact temperature with a critical magnitude. This critical magnitude of the contact temperature can be evaluated from any gear scuffing test, or can be provided by field investigations.

For a reliable evaluation of the scuffing risk, it is important that an accurate value of the gear bulk temperature be used for the analysis.

5.2 Flash temperature formula

The flash temperature formula of Blok [12][14][16][32] in a most general representation, for (approximately) band-shaped contact and tangential velocities differently directed (as for hypoid gears), see annex A, reads

$$\Theta_{fl} = 1{,}11 \cdot \frac{\mu_m \cdot X_\Gamma \cdot X_J \cdot w_{Bn}}{\sqrt{(2 \cdot b_H)}} \cdot \frac{\mathrm{abs}(v_{g1} - v_{g2})}{B_{M1} \cdot \sqrt{(v_{g1} \cdot \sin\gamma_1)} + B_{M2} \cdot \sqrt{(v_{g2} \cdot \sin\gamma_2)}} \tag{3}$$

For cylindrical or bevel gears, with band-shaped contact and parallel tangential velocities, the general representation, see annex A, reads

$$\Theta_{fl} = 1{,}11 \cdot \frac{\mu_m \cdot X_\Gamma \cdot X_J \cdot w_{Bn}}{\sqrt{(2 \cdot b_H)}} \cdot \frac{\mathrm{abs}(v_{g1} - v_{g2})}{B_{M1} \cdot \sqrt{(v_{g1})} + B_{M2} \cdot \sqrt{v_{g2}}} \tag{4}$$

or, in an equivalent representation,

$$\Theta_{fl} = 2{,}52 \cdot \mu_m \cdot \frac{X_M}{50} \cdot X_J \cdot \sqrt[4]{(X_\Gamma \cdot w_{Bt})^3} \cdot \sqrt{\left(\frac{n_1}{60}\right)} \cdot \frac{\mathrm{abs}\left(\sqrt{\rho_{y1}} - \sqrt{\rho_{y2}\,/\,u}\right)}{\sqrt[4]{\rho_{yrel}}} \tag{5}$$

where

μ_m is the mean coefficient of friction (see clause 6);

X_M is the thermo-elastic factor (see annex A);

X_M = 50 $K \cdot N^{-3/4} \cdot s^{1/2} \cdot m^{-1/2} \cdot mm$ for commonly applied steel;

X_J is the approach factor (see clause 8);

X_Γ is the load sharing factor (see clause 9);

w_{Bt} is the transverse unit load (see 5.3), in N/mm;

n_1 is the rotational speed of pinion, in r/min;

ρ_{yrel} is the local relative radius of curvature, in mm:

$$\rho_{yrel} = \frac{\rho_{y1} \cdot \rho_{y2}}{\rho_{y1} + \rho_{y2}} \tag{6}$$

ρ_{y1} is the local radius of curvature of pinion flank, in mm:

$$\rho_{y1} = \frac{1+\Gamma_y}{1+u} \cdot a \cdot \sin\alpha_{wt} \text{ (cylindrical gears)} \quad (7)$$

ρ_{y2} is the local radius of curvature of wheel flank, in mm:

$$\rho_{y2} = \frac{u-\Gamma_y}{1+u} \cdot a \cdot \sin\alpha_{wt} \text{ (cylindrical gears)} \quad (8)$$

For bevel gears, see equations (37) and (38).

For an adapted representation, see annex A.

Two Péclet numbers have to be sufficiently high, which is satisfied in almost all cases where scuffing may occur. For lower Péclet numbers the heat flow from the contact band into the gear teeth causes a different temperature distribution for which formulae (3) to (6) are not valid.

$$Pe_1 = \frac{v_{g1} \cdot b_H \cdot \rho_{M1} \cdot c_{M1}}{\lambda_{M1} \cdot \sin\gamma_1} > 5 \quad (9)$$

$$Pe_2 = \frac{v_{g2} \cdot b_H \cdot \rho_{M2} \cdot c_{M2}}{\lambda_{M2} \cdot \sin\gamma_2} > 5 \quad (10)$$

where

ρ_{M1} is the density of pinion material, in kg/m³;

ρ_{M2} is the density of wheel material, in kg/m³;

c_{M1} is the specific heat per unit mass of pinion, in J/(kg·K);

c_{M2} is the specific heat per unit mass of wheel, in J/(kg·K);

λ_{M1} is the heat conductivity of pinion, in N/(s·K);

λ_{M2} is the heat conductivity of wheel, in N/(s·K).

For cylindrical and bevel gears, $\sin\gamma_1 = \sin\gamma_2 = 1$.

5.3 Transverse unit load

The transverse unit load for cylindrical gears and bevel gears is

$$w_{Bt} = K_A \cdot K_v \cdot K_{B\beta} \cdot K_{B\alpha} \cdot K_{mp} \cdot \frac{F_t}{b} \text{ (cylindrical gears)} \quad (11)$$

$$w_{Bt} = K_A \cdot K_v \cdot K_{B\beta} \cdot K_{B\alpha} \cdot K_{mp} \cdot \frac{F_t}{b_{eff}} \text{ (bevel gears)} \quad (12)$$

where

F_t is the nominal tangential force on pitch circle, in N;

b is the facewidth, in mm;

$$b_{eff} = 0{,}85b \quad (13)$$

K_A is the application factor (see ISO 6336-1 for cylindrical gears, ISO 10300-1 for bevel gears);

K_v is the dynamic factor (see ISO 6336-1 for cylindrical gears, ISO 10300-1 for bevel gears);

$K_{B\beta}$ is the face load factor;

$K_{B\beta} = K_{H\beta}$ (see ISO 6336-1 for cylindrical gears, ISO 10300-1 for bevel gears); (14)

$K_{B\alpha}$ is the transverse load factor:

$K_{B\alpha} = K_{H\alpha}$ (see ISO 6336-1 for cylindrical gears, ISO 10300-1 for bevel gears); (15)

K_{mp} is the multiple-path factor:

The multiple-path factor K_{mp} accounts for the maldistribution in multiple-path transmissions depending on accuracy and flexibility of the branches. If no relevant analysis is available, the following may apply.

— for epicyclical gear trains with n_p planets ($n_p \geqslant 3$)

$$K_{mp} = 1 + 0{,}25\sqrt{n_p - 3} \quad (16)$$

— for dual tandem gears with quill shaft twist Φ degrees under full load

$$K_{mp} = 1 + (0{,}2 / \Phi) \quad (17)$$

— for double helical gears with an external axial force F_{ex}

$$K_{mp} = 1 + \frac{F_{ex}}{F_t \cdot \tan\beta} \quad (18)$$

— for other cases

$K_{mp} = 1$ (19)

5.4 Distribution of overall bulk temperatures

The friction loss most typical of gear transmissions is the one caused by the meshing zone. In this source the heat is generated mainly by tooth friction. The mechanical "pumping" energy expended for sideways expulsion of superfluous oil may sometimes be far from negligible. The other unavoidable friction loss is from the bearings, either of the rolling or the sliding type. In high speed gear transmissions, sliding bearings may well generate much more frictional heat than gears. Other heat sources are oil churning and friction from seals. All the above heat sources have the following features in common:

— in each of these sources the fluid friction depends on some oil viscosity representative of the operating condition;

— all of the heat sources are thermally interconnected through transmission elements to the sinks, such as the ambient air or the cooling system.

The thermal interconnection allows calculation concepts such as:

— finite element methods for discrete components;

— bondgraph methods,

— thermal network analogue methods [18].

The interfacial bulk temperature Θ_{Mi} may be suitably averaged from the two overall bulk temperatures of the teeth in contact, Θ_{M1} and Θ_{M2}. The following formula is valid to a good approximation (at high values of the Péclet numbers):

$$\Theta_{Mi} = \frac{B_{M1} \cdot \sqrt{v_{g1}} \cdot \Theta_{M1} + B_{M2} \cdot \sqrt{v_{g2}} \cdot \Theta_{M2}}{B_{M1} \cdot \sqrt{v_{g1}} + B_{M2} \cdot \sqrt{v_{g2}}} \tag{20}$$

In a fairly wide range of the ratio $\frac{B_{M1} \cdot \sqrt{v_{g1}}}{B_{M2} \cdot \sqrt{v_{g2}}}$ a simple arithmetic average is valid to a reasonable approximation

$$\Theta_{Mi} = \frac{1}{2} \cdot (\Theta_{M1} + \Theta_{M2}) \tag{21}$$

Bulk temperatures in excess of 150 °C for long periods may have an adverse effect on the surface durability.

5.5 Rough approximation of a bulk temperature

For very rough inquiry the bulk temperature may be estimated by the sum of the oil temperature, taking into account some impediment in heat transfer for spray lubrication, and a part which depends mainly on the flash temperature, of which the maximum value is taken.

$$\Theta_M = \Theta_{oil} + 0{,}47 \cdot X_S \cdot X_{mp} \cdot \Theta_{flm} \tag{22}$$

where

X_S = 1,2 for spray lubrication;

X_S = 1,0 for dip lubrication;

X_S = 1,0 for meshes with additional spray for cooling purpose;

X_S = 0,2 for gears submerged in oil, provided sufficient cooling;

$X_{mp} = \frac{1 + n_p}{2}$ for a pinion with n_p mating gears; (23)

Θ_{flm} is the average of flash temperature along path of contact, in °C:

$$\Theta_{flm} = \frac{\int_A^E \Theta_{fl} \cdot d\Gamma_y}{\Gamma_E - \Gamma_A} \tag{24}$$

However, for a reliable evaluation of the scuffing risk, it is important that instead of a rough approximation, an accurate value of the gear bulk temperature be used for the analysis.

6 Coefficient of friction

Several factors influencing the friction between gear teeth vary throughout a meshing cycle. On one of the two mating tooth faces the relative motion is uniformly accelerating, on the other it is uniformly decelerating. Only at pitch point position pure rolling occurs. In any other meshing position combined rolling and sliding will occur. Also the load acting on two mating tooth faces will vary from one meshing position to another. These conditions cause a continuous variation of the film thickness, the lubrication regime and the coefficient of friction. Even in a similar meshing position the coefficient of friction may vary for different teeth and different time.

The local coefficient of friction is considered to be a representative quantity valid for the local point concerned, smoothing various influences. The geometrically determined variation of the local coefficient of friction is difficult to calculate or to measure, hence instead of a local value, a representative mean value of the coefficient of friction will be applied.

A mean value (along the path of contact) of the coefficient of friction has commonly been applied, and even that value is uncertain. Too often, in test reports on friction, important influential quantities were neglected, for instance the bulk temperature which determines the inlet viscosity and therefore the lubrication regime.

The mean coefficient of friction[3] μ_m depends on the geometry of the path of contact, the tangential velocities, the normal load, the inlet viscosity (which is identical with viscosity at teeth bulk temperature), the pressure-viscosity coefficient, the reduced modulus of elasticity, the surface roughness, the normal relative radius of curvature. Depending on further investigations, other quantities and influences may have to be accounted for either in the formula or in the description of the field of application. The number of quantities may be reduced by dimension analysis [33], and a possible neglect of some minor influential quantities.

The coefficient of friction may be measured or estimated according to various methods. The limiting contact temperature shall be chosen correspondingly to the coefficient of friction.

6.1 Mean coefficient of friction, method A

The coefficient of friction at the onset of scuffing may be measured in gear tests or pin-and-ring tests. The limiting contact temperature is correspondingly high.

6.2 Mean coefficient of friction, method B

According to previous practice, whereby low coefficients of friction of regular working conditions are used, the final calculation of the coefficient of friction may be made with some appropriate formula, i.e. one containing a value of absolute (dynamic) viscosity η_L that corresponds to the gear bulk temperature. The limiting contact temperature is correspondingly low, see clause 10.

6.3 Mean coefficient of friction, method C

If at the start of a calculation the bulk temperature is not yet known, the mean coefficient of friction of common working conditions may be estimated by

$$\mu_m = 0{,}060 \cdot \left(\frac{w_{Bt}}{v_{g\Sigma C} \cdot \rho_{relC}} \right)^{0{,}2} \cdot X_L \cdot X_R \qquad (25)$$

where

w_{Bt} is the transverse unit load, see equation (11) or (12), in N/mm;

$v_{g\Sigma C}$ is the sum of tangential velocities in pitch point, in m/s:

$$v_{g\Sigma C} = 2 \cdot v_t \cdot \sin \alpha_{wt} \qquad (26)$$

v_t is the pitch line velocity, in m/s (if $v_t > 50$ m/s, substitute the value 50 in equation (26), instead of v_t);

ρ_{relC} is the transverse relative radius of curvature, in mm (see equation (6) for $\Gamma_y = 0$);

3) The mean coefficient of friction is defined as the mean value of the local coefficients of friction along the path of contact. Although the actual local coefficient of friction at the pitch point will differ from the mean coefficient of friction defined for the whole path of contact, that mean coefficient of friction may be expressed in terms related to the pitch point.

X_L is the lubricant factor:

$X_L = 1{,}0 \cdot (\eta_{oil})^{-0{,}05}$ for mineral oils;

$X_L = 0{,}6 \cdot (\eta_{oil})^{-0{,}05}$ for water soluble polyglycols;

$X_L = 0{,}7 \cdot (\eta_{oil})^{-0{,}05}$ for non water soluble polyglycols; (27)

$X_L = 0{,}8 \cdot (\eta_{oil})^{-0{,}05}$ for polyalfaolefins;

$X_L = 1{,}3 \cdot (\eta_{oil})^{-0{,}05}$ for phosphate esters;

$X_L = 1{,}5 \cdot (\eta_{oil})^{-0{,}05}$ for traction fluids;

η_{oil} is the dynamic viscosity at oil temperature Θ_{oil}, in mPa·s;

X_R is the roughness factor:

$$X_R = \left(\frac{Ra_1 + Ra_2}{2} \right)^{0{,}25} \quad (28)$$

where

Ra_1 is the tooth flank surface roughness, Ra, of pinion, for newly manufactured gears, in µm (for adequately run-in gears Ra_1 may reduce to about 60 % of its initial value);

Ra_2 is the tooth flank surface roughness, Ra, of wheel, for newly manufactured gears, in µm (for adequately run-in gears Ra_2 may reduce to about 60 % of its initial value).

7 Parameter on the line of action

The points on the line of action are indicated by a dimensionless linear parameter Γ_y, with the value –1 in the tangent point on the pinion base circle and the value 0 in the pitch point [33]; see Figure 3.

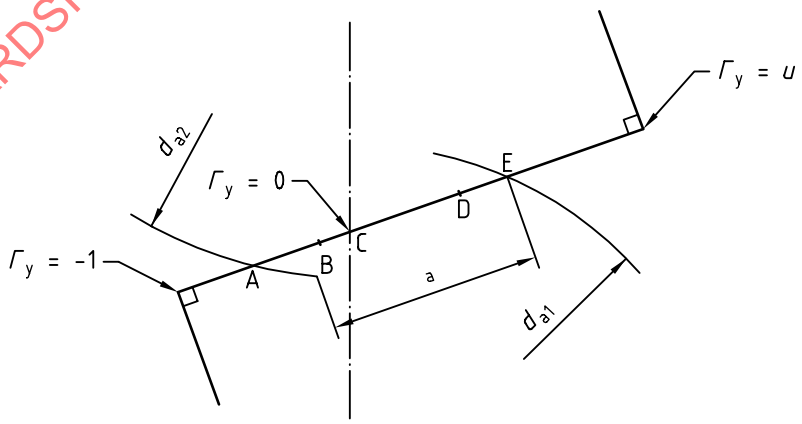

[a] Base pitch

Figure 3 — Parameter on the line of action

At an arbitrary point on the path of contact,

$$\Gamma_y = \frac{\tan\alpha_{y1}}{\tan\alpha_{wt}} - 1 \tag{29}$$

At the lower end point of the path of contact,

$$\Gamma_A = -\frac{z_2}{z_1} \cdot \left(\frac{\tan\alpha_{a2}}{\tan\alpha_{wt}} - 1 \right) \tag{30}$$

At the lower point of single pair tooth contact,

$$\Gamma_B = \frac{\tan\alpha_{a1}}{\tan\alpha_{wt}} - 1 - \frac{2 \cdot \pi}{z_1 \cdot \tan\alpha_{wt}} \tag{31}$$

At the upper point of single pair tooth contact,

$$\Gamma_D = -\frac{z_2}{z_1} \cdot \frac{\tan\alpha_{a2}}{\tan\alpha_{wt}} - 1 + \frac{2 \cdot \pi}{z_1 \cdot \tan\alpha_{wt}} \tag{32}$$

At the upper end point of the path of contact,

$$\Gamma_E = \frac{\tan\alpha_{a1}}{\tan\alpha_{wt}} - 1 \tag{33}$$

where the tip pressure angles are defined by

$$\tan\alpha_{a1} = \sqrt{\left(\frac{d_{a1}}{d_1 \cdot \cos\alpha_t} \right)^2 - 1} \tag{34}$$

$$\tan\alpha_{a2} = \sqrt{\left(\frac{d_{a2}}{d_2 \cdot \cos\alpha_t} \right)^2 - 1} \tag{35}$$

The parameters of bevel gears either may be calculated with the geometry of virtual quantities, see ISO 10300-1:—, annex A, or with the following formulae (valid also if the shaft angle $\Sigma = \delta_1 + \delta_2$ is not equal to 90°).

At an arbitrary point on the path of contact,

$$\Gamma_y = \frac{\tan\alpha_{y1}}{\tan\alpha_t} - 1 \tag{36}$$

$$\rho_{y1} = R_m \cdot \tan\delta_1 \cdot \sin\alpha_t \cdot (1 + \Gamma_y) \tag{37}$$

$$\rho_{y2} = R_m \cdot \tan\delta_1 \cdot \sin\alpha_t \cdot (u - \Gamma_y) \tag{38}$$

At marked points of the path of contact,

$$\Gamma_A = -\frac{\tan\delta_2}{\tan\delta_1} \cdot \left(\frac{\tan\alpha_{a2}}{\tan\alpha_t} - 1 \right) \tag{39}$$

$$\Gamma_B = \frac{\tan\alpha_{a1}}{\tan\alpha_t} - 1 - \frac{2 \cdot \pi \cdot \cos\delta_1}{z_1 \cdot \tan\alpha_t} \tag{40}$$

$$\Gamma_D = -\frac{\tan\delta_2}{\tan\delta_1}\cdot\left(\frac{\tan\alpha_{a2}}{\tan\alpha_t}-1\right)+\frac{2\cdot\pi\cdot\cos\delta_1}{z_1\cdot\tan\alpha_t} \quad (41)$$

$$\Gamma_E = \frac{\tan\alpha_{a1}}{\tan\alpha_t}-1 \quad (42)$$

where the tip pressure angles are defined by

$$\tan\alpha_{a1} = \sqrt{\left(\frac{\cos\alpha_t}{1+h_{am1}\cdot\cos\delta_1 / r_{m1}}\right)^2-1} \quad (43)$$

$$\tan\alpha_{a2} = \sqrt{\left(\frac{\cos\alpha_t}{1+h_{am2}\cdot\cos\delta_2 / r_{m2}}\right)^2-1} \quad (44)$$

where

δ_1 is the pitch cone angle of pinion;

δ_2 is the pitch cone angle of wheel;

R_m is the cone distance of mean cone (midface of teeth), in mm;

h_{am1} is the tip height in mean cone of pinion, in mm;

h_{am2} is the tip height in mean cone of wheel, in mm;

r_{m1} is the pitch radius in mean cone of pinion, in mm;

r_{m2} is the pitch radius in mean cone of wheel, in mm.

8 Approach factor

The approach factor takes empirically into account an increased scuffing risk in the beginning of the approach path, due to mesh starting without any previously built up oil film. Its influence is relatively strong for large gears.

The approach factor is,

— if the pinion drives the wheel (speed reducing),

$X_J = 1$ for $\Gamma_y \geqslant 0$ (45)

$$X_J = 1+\frac{C_{eff}-C_{a2}}{50}\cdot\left(\frac{-\Gamma_y}{\Gamma_E-\Gamma_A}\right)^3, \text{ provided } X_J \geqslant 1, \text{ for } \Gamma_y < 0 \quad (46)$$

— if the wheel drives the pinion (speed increasing),

$X_J = 1$ for $\Gamma_y \leqslant 0$ (47)

$$X_J = 1+\frac{C_{eff}-C_{a1}}{50}\cdot\left(\frac{\Gamma_y}{\Gamma_E-\Gamma_A}\right)^3, \text{ provided } X_J \geqslant 1, \text{ for } \Gamma_y > 0 \quad (48)$$

where

C_{eff} is the optimal tip relief (see annex B), in μm;

C_{a1} is the tip relief of pinion, μm;

C_{a2} is the tip relief of wheel, μm;

Γ_y is the parameter of arbitrary point (see clause 7);

Γ_A is the parameter of point A (see clause 7);

Γ_E is the parameter of point B (see clause 7);

9 Load sharing factor

The load sharing factor X_Γ accounts for the load sharing of succeeding pairs of meshing teeth. By convention, the load sharing factor is presented as a function of the linear parameter Γ_y on the path of contact, increasing at the approach path of transverse double contact, when the preceding pair of meshing teeth ends its action, and decreasing at the recess path of transverse double contact, when the succeeding pair of meshing teeth comes into action.

Due to inaccuracies a preceding pair of meshing teeth may cause an instantaneous increase or decrease of the theoretical load sharing factor, independent of the instantaneous increase or decrease caused by inaccuracies of a succeeding pair of meshing teeth at a later time.

The value of X_Γ does not exceed 1,00 (for cylindrical gears), which means full transverse single tooth contact. The region of transverse single tooth contact may be extended by an irregularly varying location of a dynamic load.

The load sharing factor X_Γ depends on the type of gear transmission and on the profile modification. In case of buttressing of helical teeth (undersized profile modification), the load sharing factor is combined with a buttressing factor X_{but}.

Formulae for profile modification (tip relief) are given in annex B.

9.1 Buttressing factor

Helical gears may have a buttressing effect near the end points A and E of the line of action, due to the oblique contact lines. This applies to both cylindrical and bevel gears with tip relief less than an optimum value, $C_a < C_{eff}$.

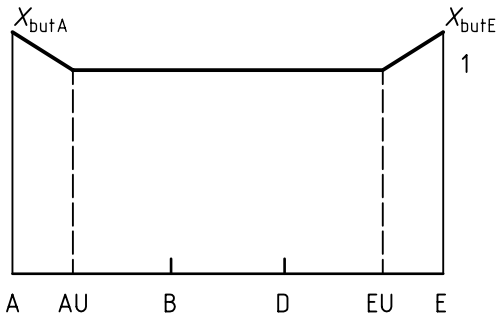

Figure 4 — Buttressing function

The buttressing is expressed by means of a factor X_{but}, simplified as linear functions within the ranges A-AU, AU-EU, EU-E; see Figure 4, marked by the following values:

$$\Gamma_{AU} - \Gamma_A = \Gamma_E - \Gamma_{EU} = 0{,}2 \cdot \sin\beta_b \quad \text{for cylindrical gears} \tag{49}$$

$$\Gamma_{AU} - \Gamma_A = \Gamma_E - \Gamma_{EU} = 0{,}2 \cdot \sin\beta_{bm} \quad \text{for bevel gears} \tag{50}$$

$$X_{butA} = X_{butE} = 1{,}3 \quad \text{when } \varepsilon_\beta \geqslant 1 \tag{51}$$

$$X_{butA} = X_{butE} = 1 + 0{,}3 \cdot \varepsilon_\beta \quad \text{when } \varepsilon_\beta < 1 \tag{52}$$

$$X_{butAU} = X_{butEU} = 1 \tag{53}$$

$$X_{but} = X_{butA} - \frac{\Gamma_y - \Gamma_A}{\Gamma_{AU} - \Gamma_A} \cdot (X_{butA} - 1) \quad \text{for } \Gamma_A \leqslant \Gamma_y < \Gamma_{AU} \tag{54}$$

$$X_{but} = 1 \quad \text{for } \Gamma_{AU} \leqslant \Gamma_y \leqslant \Gamma_{EU} \tag{55}$$

$$X_{but} = X_{butE} - \frac{\Gamma_E - \Gamma_y}{\Gamma_E - \Gamma_{EU}} \cdot (X_{butE} - 1) \quad \text{for } \Gamma_{EU} < \Gamma_y \leqslant \Gamma_E \tag{56}$$

9.2 Spur gears with unmodified profiles

The load sharing factor for a spur gear with unmodified profile is conventionally supposed to have a discontinuous trapezoidal shape; see Figure 5. However, due to manufacturing inaccuracies, in each path of double contact the load sharing factor will increase for protruding flanks and decrease for other flanks [34]. The representative load sharing factor is an envelope of possible curves; see Figure 6.

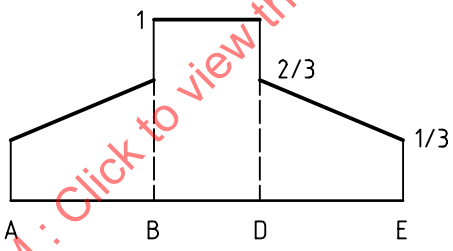

Figure 5 — Load sharing factor for cylindrical spur gears with unmodified profiles and quality grade 7 or finer

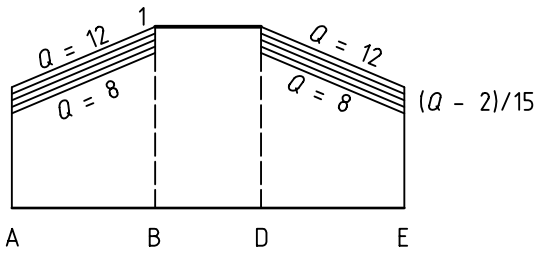

Figure 6 — Load sharing factor for cylindrical spur gears with unmodified profiles and quality grade 8 or coarser

$$X_\Gamma = \frac{Q-2}{15} + \frac{1}{3} \cdot \frac{\Gamma_y - \Gamma_A}{\Gamma_B - \Gamma_A} \quad \text{for } \Gamma_A \leqslant \Gamma_y < \Gamma_B \tag{57}$$

$$X_\Gamma = 1 \quad \text{for } \Gamma_B < \Gamma_y \leqslant \Gamma_D \tag{58}$$

$$X_\Gamma = \frac{Q-2}{15} + \frac{1}{3}\cdot\frac{\Gamma_E - \Gamma_y}{\Gamma_E - \Gamma_D} \qquad \text{for } \Gamma_D \leqslant \Gamma_y \leqslant \Gamma_E \tag{59}$$

Q = 7 for quality grade 7 or finer (60)

Q = equals quality grade for grade 8 or coarser.

9.3 Spur gears with profile modification

See Figures 7 and 8.

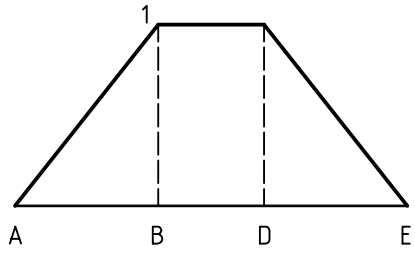

Figure 7 — Load sharing factor for cylindrical spur gears with optimal profile modification

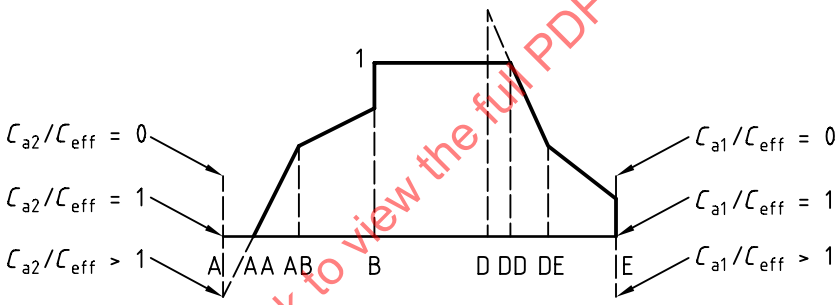

Figure 8 — Load sharing factor for cylindrical spur gears with oversized profile modification near A, and undersized profile modification near E.

$$X_\Gamma = \left(1 - \frac{C_{a2}}{C_{eff}}\right)\cdot\frac{1}{3} + \left(\frac{1}{3} + \frac{2}{3}\cdot\frac{C_{a2}}{C_{eff}}\right)\cdot\frac{\Gamma_y - \Gamma_A}{\Gamma_B - \Gamma_A} \qquad \text{provided } X_\Gamma \geqslant 0, \text{ for } \Gamma_A \leqslant \Gamma_y \leqslant \Gamma_{AB} \tag{61}$$

$$X_\Gamma = \left(1 - \frac{C_{a1}}{C_{eff}}\right)\cdot\frac{1}{3} + \left(\frac{1}{3} + \frac{2}{3}\cdot\frac{C_{a1}}{C_{eff}}\right)\cdot\frac{\Gamma_y - \Gamma_A}{\Gamma_B - \Gamma_A} \qquad \text{provided } X_\Gamma \leqslant 1, \text{ for } \Gamma_{AB} \leqslant \Gamma_y \leqslant \Gamma_B \tag{62}$$

$$X_\Gamma = 1 \qquad \text{for } \Gamma_B \leqslant \Gamma_y \leqslant \Gamma_D \tag{63}$$

$$X_\Gamma = \left(1 - \frac{C_{a2}}{C_{eff}}\right)\cdot\frac{1}{3} + \left(\frac{1}{3} + \frac{2}{3}\cdot\frac{C_{a2}}{C_{eff}}\right)\cdot\frac{\Gamma_E - \Gamma_y}{\Gamma_E - \Gamma_D} \qquad \text{provided } X_\Gamma \leqslant 1, \text{ for } \Gamma_D \leqslant \Gamma_y \leqslant \Gamma_{DE} \tag{64}$$

$$X_\Gamma = \left(1 - \frac{C_{a1}}{C_{eff}}\right)\cdot\frac{1}{3} + \left(\frac{1}{3} + \frac{2}{3}\cdot\frac{C_{a1}}{C_{eff}}\right)\cdot\frac{\Gamma_E - \Gamma_y}{\Gamma_E - \Gamma_D} \qquad \text{provided } X_\Gamma \geqslant 0, \text{ for } \Gamma_{DE} \leqslant \Gamma_y \leqslant \Gamma_D \tag{65}$$

$$\Gamma_{AB} = 0{,}5\cdot(\Gamma_A + \Gamma_B) \tag{66}$$

$$\Gamma_{DE} = 0{,}5\cdot(\Gamma_D + \Gamma_E) \tag{67}$$

$$\Gamma_{AA} = \frac{(C_{a2} + 2\cdot C_{eff})\cdot\Gamma_A + (C_{a2} - C_{eff})\cdot\Gamma_B}{2\cdot C_{a2} + C_{eff}} \qquad \text{for } C_{a2} > C_{eff} \tag{68}$$

$$\Gamma_{AA} = \Gamma_A \qquad \text{for } C_{a2} \leqslant C_{eff} \tag{69}$$

$$\Gamma_{BB} = \frac{(C_{a1} - C_{eff}) \cdot \Gamma_A + (C_{a1} + 2 \cdot C_{eff}) \cdot \Gamma_B}{2 \cdot C_{a1} + C_{eff}} \qquad \text{for } C_{a1} > C_{eff} \tag{70}$$

$$\Gamma_{BB} = \Gamma_B \qquad \text{for } C_{a1} \leqslant C_{eff} \tag{71}$$

$$\Gamma_{DD} = \frac{(C_{a2} - C_{eff}) \cdot \Gamma_E + (C_{a2} + 2 \cdot C_{eff}) \cdot \Gamma_D}{2 \cdot C_{a2} + C_{eff}} \qquad \text{for } C_{a2} > C_{eff} \tag{72}$$

$$\Gamma_{DD} = \Gamma_D \qquad \text{for } C_{a2} \leqslant C_{eff} \tag{73}$$

$$\Gamma_{EE} = \frac{(C_{a1} + 2 \cdot C_{eff}) \cdot \Gamma_E + (C_{a1} - C_{eff}) \cdot \Gamma_D}{2 \cdot C_{a1} + C_{eff}} \qquad \text{for } C_{a1} > C_{eff} \tag{74}$$

$$\Gamma_{EE} = \Gamma_E \qquad \text{for } C_{a1} \leqslant C_{eff} \tag{75}$$

9.4 Narrow helical gears with unmodified profiles

Helical gears with a small total contact ratio, $\varepsilon_\gamma < 2$, have still pure single contact of tooth pairs. Hence, they can be treated similar to spur gears, considering the geometry in the transverse plane, as well as the buttressing effect. See Figure 9.

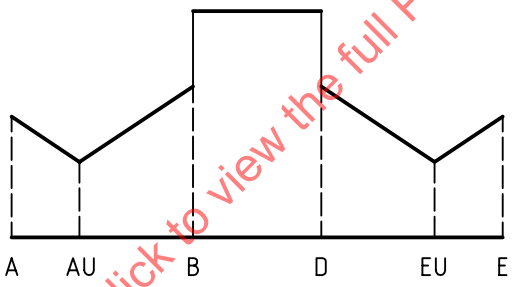

Figure 9 — Load sharing factor for narrow helical cylindrical gears with unmodified profiles, including the buttressing effect

The load sharing factor is obtained by multiplying the X_Γ in 9.2 with the buttressing factor X_{but}.

9.5 Narrow helical gears with profile modification

Helical gears with a small total contact ratio, $\varepsilon_\gamma < 2$, have still pure single contact of tooth pairs. Hence, they can be treated similar to spur gears, considering the geometry in the transverse plane. See Figures 10 and 11.

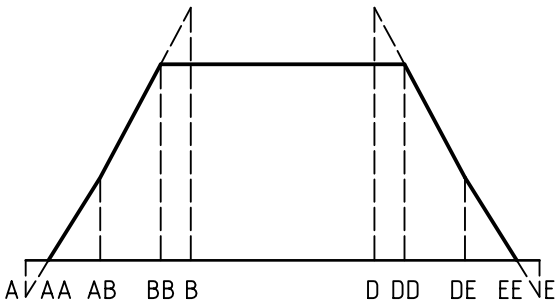

Figure 10 — Load sharing factor for narrow helical cylindrical gears with optimal or oversized profile modification

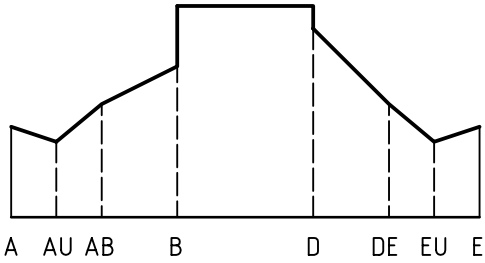

Figure 11 — Load sharing factor for narrow helical cylindrical gears with undersized profile modification

The load sharing factor is obtained by multiplying the X_Γ in 9.2 with the buttressing factor X_{but}.

9.6 Wide helical gears with unmodified profiles

The buttressing effect [35] of local high mesh stiffness at the end of oblique contact lines for wide helical gears, $\varepsilon_\gamma > 2$, is assumed to act near the ends A and E along the helix teeth over a constant length, which corresponds to a transverse relative distance $0{,}2 \sin\beta_b$; see Figure 12. See also 9.1 and Figure 4.

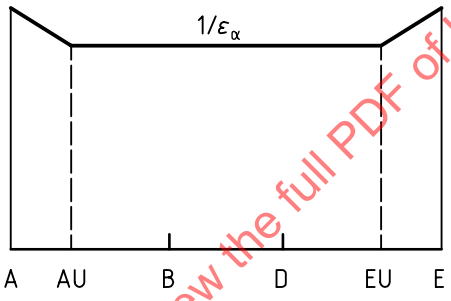

Figure 12 — Load sharing factor for wide cylindrical helical gears with unmodified profiles

The load sharing factor is obtained by multiplying the value $1/\varepsilon_\alpha$, representing the mean load, with the buttressing factor X_{but}:

$$X_\Gamma = \frac{1}{\varepsilon_\alpha} \cdot X_{\text{but}} \tag{76}$$

9.7 Wide helical gears with profile modification

The extensions of tip relief at both ends A-AB and DE-E of the path of contact are assumed to be equal and to result in a contact ratio $\varepsilon_\alpha = 1$ for unloaded gears; see Figure 13. The load sharing factor for wide cylindrical helical gears, $\varepsilon_\gamma \geqslant 2$, with undersized or with oversized profile modification follows from interpolation or extrapolation, respectively, between the factor for unmodified profile with buttressing effect and the factor for optimal profile modification; see Figure 14.

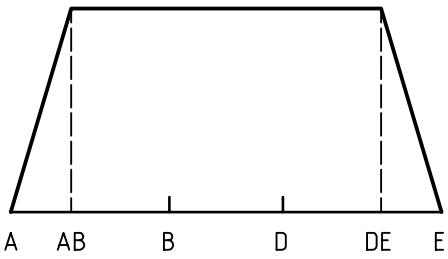

Figure 13 — Load sharing factor for wide cylindrical helical gears with optimal profile modification

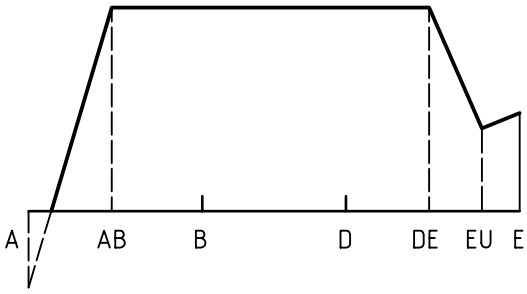

Figure 14 — Load sharing factor for wide cylindrical helical gears with oversized profile modification near A, and undersized near E

The ranges are marked by the following points

$$\Gamma_{AB} = 0{,}5 \cdot (\Gamma_A + \Gamma_B) \tag{77}$$

$$\Gamma_{DE} = 0{,}5 \cdot (\Gamma_D + \Gamma_E) \tag{78}$$

$$\Gamma_{AA} = \Gamma_A + \frac{(\varepsilon_\alpha + 1) \cdot (\varepsilon_\alpha - 1) \cdot (C_{a2} - C_{eff})}{(\varepsilon_\alpha - 1) \cdot C_{a1} + (3\varepsilon_\alpha + 1) \cdot C_{a2}} \cdot (\Gamma_E - \Gamma_A) \quad \text{for } C_{a2} \geqslant C_{eff} \tag{79}$$

$$\Gamma_{EE} = \Gamma_E + \frac{(\varepsilon_\alpha + 1) \cdot (\varepsilon_\alpha - 1) \cdot (C_{a1} - C_{eff})}{(\varepsilon_\alpha - 1) \cdot C_{a2} + (3\varepsilon_\alpha + 1) \cdot C_{a1}} \cdot (\Gamma_E - \Gamma_A) \quad \text{for } C_{a1} \geqslant C_{eff} \tag{80}$$

$$X_\Gamma = \frac{C_{eff} - C_{a2}}{\varepsilon_\alpha \cdot C_{eff}} + \frac{(\varepsilon_\alpha - 1) \cdot C_{a1} + (3\varepsilon_\alpha + 1) \cdot C_{a2}}{2 \cdot \varepsilon_\alpha \cdot (\varepsilon_\alpha + 1) \cdot C_{eff}} \cdot \frac{\Gamma_y - \Gamma_A}{\Gamma_{AB} - \Gamma_A} \quad \text{for } \Gamma_{AA} \leqslant \Gamma_y \leqslant \Gamma_{AB} \text{ if } C_{a2} < C_{eff}$$

$$\text{for } \Gamma_A \leqslant \Gamma_y \leqslant \Gamma_{AB} \text{ if } C_{a2} \geqslant C_{eff} \tag{81}$$

$$X_\Gamma = 0 \quad \text{for } \Gamma_{AA} \leqslant \Gamma_y \leqslant \Gamma_{AB} \text{ if } C_{a2} \geqslant C_{eff} \tag{82}$$

$$X_\Gamma = \frac{1}{\varepsilon_\alpha} + \frac{(\varepsilon_\alpha - 1)}{2 \cdot \varepsilon_\alpha \cdot (\varepsilon_\alpha + 1)} \cdot \frac{C_{a1} + C_{a2}}{C_{eff}} \quad \text{for } \Gamma_{AB} \leqslant \Gamma_y \leqslant \Gamma_{DE} \tag{83}$$

$$X_\Gamma = \frac{C_{eff} - C_{a1}}{\varepsilon_\alpha \cdot C_{eff}} + \frac{(\varepsilon_\alpha - 1) \cdot C_{a2} + (3\varepsilon_\alpha + 1) \cdot C_{a1}}{2 \cdot \varepsilon_\alpha \cdot (\varepsilon_\alpha + 1) \cdot C_{eff}} \cdot \frac{\Gamma_E - \Gamma_y}{\Gamma_E - \Gamma_{DE}} \quad \text{for } \Gamma_{DE} \leqslant \Gamma_y \leqslant \Gamma_E \text{ if } C_{a1} < C_{eff}$$

$$\text{for } \Gamma_{DE} \leqslant \Gamma_y \leqslant \Gamma_{EE} \text{ if } C_{a1} \geqslant C_{eff} \tag{84}$$

$$X_\Gamma = 0 \quad \text{for } \Gamma_{DE} \leqslant \Gamma_y \leqslant \Gamma_{EE} \text{ if } C_{a1} \geqslant C_{eff} \tag{85}$$

9.8 Narrow bevel gears

For narrow bevel gears, $\varepsilon_\gamma < 2$, with profile modification $C_a < C_{eff}$, the load sharing factor X_Γ is found by linear interpolation between X_Γ as calculated (for $C_a = 0$) in 9.4, and X_Γ as calculated (for $C_a = C_{eff}$) in 9.9. Remember X_{but}.

For narrow bevel gears, $\varepsilon_\gamma < 2$, with profile modification $C_a \geqslant C_{eff}$, the load sharing factor X_Γ is calculated as in 9.9.

9.9 Wide bevel gears

For wide bevel gears, $\varepsilon_\gamma \geqslant 2$, with optimal profile modification, $C_{a1} = C_{eff}$, $C_{a2} = C_{eff}$, the load sharing factor is assumed to be parabolic [35]; see Figure 15.

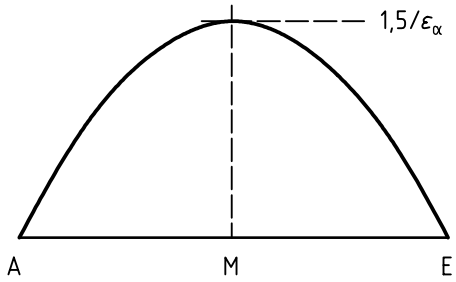

Figure 15 — Load sharing factor for bevel gears with optimal profile modification

The midpoint M is defined by

$$\Gamma_M = \frac{\Gamma_A + \Gamma_E}{2} \tag{86}$$

The load sharing factor for optimal profile modification is

$$X_\Gamma = \frac{1{,}5}{\varepsilon_\alpha} - \frac{(\Gamma_y - \Gamma_M)^2}{(\Gamma_E - \Gamma_A)^2} \cdot \frac{6}{\varepsilon_\alpha} \qquad \text{for } C_{a1} = C_{eff},\ C_{a2} = C_{eff} \tag{87}$$

If the profile modification C_{a1} differs from C_{a2}, then the sections AM and ME shall be calculated separately with a discontinuity at point M; see Figure 16.

For undersized profile modification an interpolation is made between the factor for unmodified profile with buttressing effect according to 9.6, and the parabola for optimal profile modification.

For oversized profile modification the parabola has a new end point AA or EE.

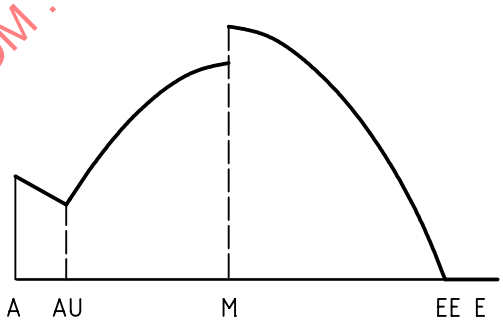

Figure 16 — Load sharing factor for bevel gears with undersized profile modification near A and oversized profile modification near E

For undersized profile modification, X_Γ is found by linear interpolation between X_Γ for optimal profile modification, equation (87), and X_Γ for unmodified profile according to equation (76). This interpolation is to be made stepwise from A to M with the influence of C_{a2}, and from M to E with the influence of C_{a1}.

For oversized profile modification, new end points AA and EE are found as

$$\Gamma_{AA} = \Gamma_A + \frac{\varepsilon_\alpha}{6} \cdot (\Gamma_E - \Gamma_A) \cdot \left(\frac{C_{a2}}{C_{eff}} - 1 \right) \tag{88}$$

$$\Gamma_{EE} = \Gamma_E - \frac{\varepsilon_\alpha}{6} \cdot (\Gamma_E - \Gamma_A) \cdot \left(\frac{C_{a1}}{C_{eff}} - 1 \right) \tag{89}$$

$$X_\Gamma = 0 \qquad \text{for } \Gamma_A \leqslant \Gamma_y \leqslant \Gamma_{AA} \tag{90}$$

$$X_\Gamma = \frac{1{,}5}{\varepsilon_\alpha} \cdot \frac{3}{4 - C_{a2} / C_{eff}} \cdot \left\{ 1 - \frac{(\Gamma_y - \Gamma_M)^2}{(\Gamma_{AA} - \Gamma_M)^2} \right\} \qquad \text{for } \Gamma_{A\,A} < \Gamma_A \leqslant \Gamma_M \tag{91}$$

$$X_\Gamma = \frac{1{,}5}{\varepsilon_\alpha} \cdot \frac{3}{4 - C_{a1} / C_{eff}} \cdot \left\{ 1 - \frac{(\Gamma_y - \Gamma_M)^2}{(\Gamma_{EE} - \Gamma_M)^2} \right\} \qquad \text{for } \Gamma_M \leqslant \Gamma_y < \Gamma_{EE} \tag{92}$$

$$X_\Gamma = 0 \qquad \text{for } \Gamma_{EE} \leqslant \Gamma_y \leqslant \Gamma_E \tag{93}$$

10 Scuffing temperature and safety

10.1 Scuffing temperature

The scuffing temperature is the contact temperature at which scuffing is likely to occur with the chosen combination of lubricant and gear materials. The scuffing temperature is assumed to be a characteristic value for the material-lubricant-material system of a gear pair, to be determined by gear tests with the same material-lubricant-material system [36].

When using a low-additive mineral oil, the scuffing temperature is assumed to be independent of operating conditions in a fairly wide range.

When using a mineral oil or a synthetic oil with anti-scuff or friction-reducing additives, extended research is still needed to determine the nature of a possible non-constancy of the scuffing temperature for the materials and the operating conditions concerned. Special attention shall be paid to the correlation between test conditions and actual or design conditions. The correlation may be strongly influenced by properties shown in the transition diagram; see Figure 1.

10.2 Structural factor

The scuffing temperature of low-additive mineral oils that is determined from test gears may be extended to different gear steels, heat treatments or surface treatments by introducing an empirical structural factor.

$$\Theta_S = \Theta_{MT} + X_W \cdot \Theta_{flmaxT} \tag{94}$$

where

Θ_{MT} is the bulk temperature of test gears, in °C;

Θ_{flmaxT} is the maximum flash temperature of test gears, in K;

X_W is the structural factor (see Table 2).

Table 2 — Structural factor

Material	X_W
Through-hardened steel	1,00
Phosphated steel	1,25
Copper-plated steel	1,50
Bath or gas nitrided steel	1,50
Hardened carburized steel, with austenite content:	
— less than average	1,15
— average (10 % to 20 %)	1,00
— greater than average	0,85
Austenite steel (stainless steel)	0,45

However, this approximation is restricted to methods using the coefficient of friction for common working conditions (see 6.3) together with an average value of the thermo-elastic factor (see clause 8). The structural factor may be superfluous if methods are used considering realistic values of the coefficient of friction and the thermo-elastic factor.

10.3 Contact exposure time

It was shown by tests [37] that the scuffing temperature of gears lubricated with anti-scuff oils may be influenced by the contact exposure time, that is the time during which a point on a tooth flank is exposed to the Hertzian contact band of the meshing tooth.

The decisive contact exposure time t_{max} for a pair of tooth flanks is the longest of t_1 and t_2

$$t_{max} \geqslant t_1 = \frac{2 \cdot b_H}{v_{g1}} \tag{95}$$

$$t_{max} \geqslant t_2 = \frac{2 \cdot b_H}{v_{g2}} \tag{96}$$

The dependence of the scuffing temperature Θ_S on the contact time is approximated as shown in Figure 17 by a curve consisting of two straight lines

$$\Theta_S = \Theta_{Sc} + X_\Theta \cdot X_W \cdot (t_c - t_{max}) \qquad \text{for } t_{max} < t_c \tag{97}$$

$$\Theta_S = \Theta_{Sc} \qquad \text{for } t_{max} \geqslant t_c \tag{98}$$

where

Θ_{Sc} is the scuffing temperature at long contact times, in °C;

X_Θ is the gradient of the scuffing temperature, in K/μs;

X_W is the structural factor;

t_c is the contact exposure time at the bend of the curve, in μs;

t_{max} is the contact exposure time of meshing teeth, in μs.

The following values may be applied for oils:

— without anti-scuff additives: X_Θ = 0 K/µs, t_c = 0 µs;

— with anti-scuff additives: X_Θ = 18 K/µs, t_c = 18 µs.

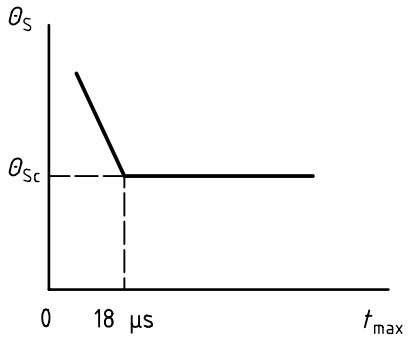

Figure 17 — Influence of contact exposure time on the scuffing temperature for anti-scuff oils

10.4 Scuffing temperature in gear tests

The scuffing temperature may be determined in gear tests, such as Ryder [38], FZG-Ryder [39], FZG L-42 [40], FZG A/8,3/90 [41].

The test result shall be expressed in a scuffing temperature, together with the test conditions. If the test result is expressed in other terms, then a relation shall be given as, for instance:

$$\Theta_S = 80 + (0{,}85 + 1{,}4 \cdot X_W) \cdot X_L \cdot (S_{FZG})^2 \qquad (99)$$

where

X_W is the structural factor (see Table 2);

X_L is the lubricant factor, [see equation (27)];

S_{FZG} is the load stage according to FZG A/8,3/90 test. This is the load stage where scuffing occurs.

However, oil data tend to vary much with regard to S_{FZG}, a load stage variation of ± 1 is common, and it is assumed that the oil somewhat deteriorates during an oil shift interval. Therefore, calculations may be made with one load stage less than the specification.

10.5 Safety range

In contrast to the long time for development of fatigue damage, a single momentary overload can initiate scuffing of such severity that affected gears may not longer be fit for use. This should be carefully considered when choosing an adequate safety range, especially for gears required to operate with high pitch line velocities.

In cases with a short contact exposure time t_{max} and safety conditions based on an increased scuffing temperature $\Theta_S > \Theta_{Sc}$ (see 10.3) that contact exposure time t_{max} shall not increase, unless the transmitted power is lowered adequately.

A safety factor may be defined by

$$S_B = \frac{\Theta_S - \Theta_{oil}}{\Theta_{Bmax} - \Theta_{oil}} \qquad (100)$$

where

Θ_S is the scuffing temperature, in °C;

Θ_{Bmax} is the maximum contact temperature, in °C;

Θ_{oil} is the oil temperature, in °C.

However, the relation between the actual gear load and the decisive contact temperature is very complicated, and the use of a safety factor expressed in any quotient of temperatures may cause confusion.

Therefore, in addition to the specification of the test load stage (see 10.4) it is advised to express the concept of safety as a demanded minimum difference (for instance $\geqslant$ 50 K) between the scuffing temperature and the estimated maximum contact temperature.

Annex A
(informative)

Flash temperature formula presentation

Since the first publication of the original flash temperature formula [12] [14] Blok made the following conversions:

— step from width to semi-width of Hertzian contact band and substitution of $0{,}83 \cdot \sqrt{2} = 1{,}17$ for parabolic friction heat distribution by 1,11 for elliptic friction heat distribution [16];

— extension to unequally directed tangential velocities [32]; see equation (3).

For convenience, exact conversions were made:

— some quantities were expressed in other quantities, for instance the semi-width of Hertzian contact band and the radii of curvature;

— some parts of the formula were concentrated in separate factors, for instance the thermo-elastic factor; see clause A.3.

For practical applications adaptive conversions were made:

— redefinition of factors, for instance the load sharing factor; see clause 9;

— addition of empirical factors, for instance the approach factor; see clause 8.

A.1 General case

In a most general case of tooth contact (e.g. hypoid gears) the successive contact areas will assume the shape of tapered bands; see Figure A.1. Moreover, the two tangential velocities, v_{g1} and v_{g2}, are directed at unequal angles, γ_1 and γ_2, with respect to the longitudinal axis of such an area. In simpler cases (e.g. cylindrical gears) the angles reduce into $\gamma_1 = \gamma_2 = \pi/2$.

The distribution of the contact pressures over some cross-section in a tapered contact area may be approximated by the semi-elliptical distribution that would occur over a substitute band-shaped contact area interposed between two parallel surfaces, whilst having a uniform width equal to the aforementioned local width; see Figure A.1.

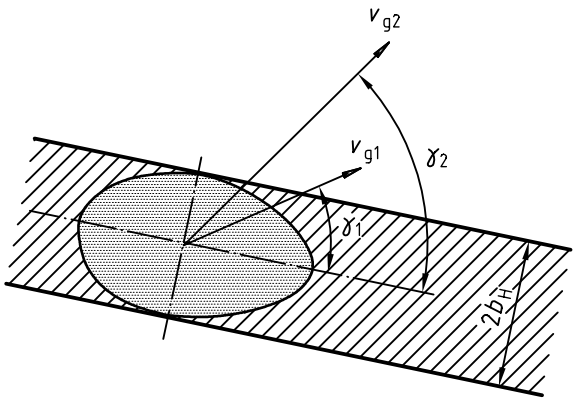

Figure A.1 — Substitute band-shaped contact area, with two tangential velocities in different directions

The actual Hertzian contact zone of hypoid gears may be supposed to be elliptical and the tangential velocities are neither coincident nor perpendicular to a major axis of the contact zone. However, the elliptical contact may be rather elongated in having a sufficiently high elliptical ratio, or it may have the shape of a somewhat tapered band.

Either tangential velocity is to show a direction deviating not too much from that of the minor axis. In other words, let either velocity have a component along the major axis.

For determining the maximum flash temperature sought, the actual elliptic contact zone may be substituted by a band-shaped contact zone of which the width $2\,b_H$ equals the length of the minor axis of the ellipse; see Figure A.1.

Note that the maximum contact pressure here, like the minor axis, may be directly proportional to the cubic root of the load, instead of the square root. In some cases, the Hertzian formulae have to be adapted for elongated point contact [42].

To summarize, the present procedure would appear justifiable to a reasonable approximation. A major reason lies in the feature that, for the actual sufficiently elongated elliptic contacts under the above-defined kinematic conditions, one may expect the actual maximum flash temperature to occur at a point fairly close to the minor axis concerned.

The flash temperature formula of Blok [12][14][16][32] for substitute band-shaped contact and tangential velocities differently directed is

$$\Theta_{fl} = 1{,}11 \cdot \frac{\mu_m \cdot X_J \cdot X_\Gamma \cdot w_{Bn} \cdot \mathrm{abs}\left(v_{g1} - v_{g2}\right)}{\left(2 \cdot b_H\right)^{1/2} \cdot B_{M1} \cdot \left(v_{g1} \cdot \sin\gamma_1\right)^{1/2} + B_{M2} \cdot \left(v_{g2} \cdot \sin\gamma_2\right)^{1/2}} \qquad \text{(A.1)}$$

where

μ_m is the mean coefficient of friction;

X_J is the approach factor, see clause 8;

X_Γ is the load sharing factor, see clause 9;

w_{Bn} is the normal unit load, in N/mm:

$$w_{Bn} = \frac{w_{Bt}}{\cos\alpha_{wn} \cdot \cos\beta_w} \qquad \text{(A.2)}$$

where

w_{Bt} is the transverse unit load, see 5.3, in N/mm;

α_{wn} is the normal working pressure angle, in degrees:

$$\alpha_{wn} = \arcsin\left(\sin\alpha_{wt} \cdot \cos\beta_b\right) \qquad \text{(A.3)}$$

β_w is the working helix angle, in degrees:

$$\beta_w = \arctan\left(\frac{\tan\beta_b}{\cos\alpha_{wt}}\right) \qquad \text{(A.4)}$$

b_H is the semi-width of Hertzian contact band, in mm;

v_{g1} is the tangential velocity (vector) of pinion, in m/s;

v_{g2} is the tangential velocity (vector) of wheel, in m/s;

B_{M1} is the thermal contact coefficient of pinion, see clause A.3, in N/(mm$^{1/2}$·m$^{1/2}$·s$^{1/2}$·K);

B_{M2} is the thermal contact coefficient of wheel, see clause A.3, in N/(mm$^{1/2}$·m$^{1/2}$·s$^{1/2}$·K);

γ_1 is the angle of direction of tangential velocity of pinion, in degrees;

γ_2 is the angle of direction of tangential velocity of wheel, in degrees.

A.2 Cylindrical gears

The flash temperature formula adapted[4] for cylindrical gears reads

$$\Theta_{fl} = \mu_m \cdot X_M \cdot X_J \cdot X_G \cdot \left(X_\Gamma \cdot w_{Bt}\right)^{3/4} \cdot \frac{v_t^{1/2}}{a^{1/4}} \qquad \text{(A.5)}$$

where

μ_m is the mean coefficient of friction (see clause 6);

X_M is the thermo-elastic factor (see clause A.3);

X_J is the approach factor (see clause 8);

X_G is the geometry factor

for an external gear pair:

$$X_G = 0{,}51 \cdot X_{\alpha\beta} \cdot (u+1)^{1/2} \cdot \frac{\text{abs}\left(1+\Gamma_y - 1 - \Gamma_y / u\right)}{(1+\Gamma_y)^{1/4} \cdot (u-\Gamma_y)^{1/4}} \qquad \text{(A.6)}$$

for an internal gear pair (practical sign convention):

$$X_G = 0{,}51 \cdot X_{\alpha\beta} \cdot (u-1)^{1/2} \cdot \frac{\text{abs}\left(1+\Gamma_y - 1 + \Gamma_y / u\right)}{\left(1+\Gamma_y\right)^{1/4} \cdot \left(u+\Gamma_y\right)^{1/4}} \qquad \text{(A.7)}$$

X_Γ is the load sharing factor (see clause 9);

w_{Bt} is the transverse unit load (see 5.3);

v_t is the pitch line velocity;

a is the centre distance.

4) To avoid possible misinterpretation of the unit of the rotational frequency, the formula is expressed in pitch line velocity and centre distance, instead of more logically the rotational frequency and centre distance. The old-fashioned interpretation of n is revolutions per minute with the unit r/min. Any attempt to redefine "revolutions per time" in order to obtain a coherent system of units fails, since the unit 1/s has a double meaning, either 360°-angle/s or radian/s. The deeper cause of this ambiguity in the international system of units is a lacking dimension for the quantity angle and an ill-considered omission of the unit radian in too many cases. The solution is to reduce the "quantity" revolution into the "phenomenon" rotational frequency with the frequency unit Hz.